arXiv:2505.05007v1 [cs.CV] 8 May 2025

Driving with Context: Online Map Matching for Complex Roads Using Lane Markings and Scenario Recognition

Xin Bi[1], Zhichao Li[1], Yuxuan Xia[2], Panpan Tong[1], Lijuan Zhang[2], Yang Chen[2], and Junsheng Fu[2]

***Abstract*— Accurate online map matching is fundamental to vehicle navigation and the activation of intelligent driving functions. Current online map matching methods are prone to errors in complex road networks, especially in multilevel road area. To address this challenge, we propose an online Standard Definition (SD) map matching method by constructing a Hidden Markov Model (HMM) with multiple probability factors. Our proposed method can achieve accurate map matching even in complex road networks by carefully leveraging lane markings and scenario recognition in the designing of the probability factors. First, the lane markings are generated by a multi-lane tracking method and associated with the SD map using HMM to build an enriched SD map. In areas covered by the enriched SD map, the vehicle can re-localize itself by performing Iterative Closest Point (ICP) registration for the lane markings. Then, the probability factor accounting for the lane marking detection can be obtained using the association probability between adjacent lanes and roads. Second, the driving scenario recognition model is applied to generate the emission probability factor of scenario recognition, which improves the performance of map matching on elevated roads and ordinary urban roads underneath them. We validate our method through extensive road tests in Europe and China, and the experimental results show that our proposed method effectively improves the online map matching accuracy as compared to other existing methods, especially in multilevel road area. Specifically, the experiments show that our proposed method achieves F_1 scores of 98.04% and 94.60% on the Zenseact Open Dataset and test data of multilevel road areas in Shanghai respectively, significantly outperforming benchmark methods. The implementation is available at github.com/TRV-Lab/LMSR-OMM.**

***Index Terms*— Map matching, Hidden Markov Model, lane marking map, driving scenario recognition**

I. INTRODUCTION

Intelligent driving functions usually require a well defined operational design domain (ODD) [1], and online map matching enables vehicles to assess whether they are traversing areas and road classes that fall within the ODD for intelligent driving functions. Map matching errors can disrupt navigation systems and erroneously deactivate intelligent driving functions, affecting vehicle trajectory planning and speed control, increasing accident risks.

This work was completed with the support of the collaboration between Zenseact and Tongji University. Zhichao Li accessed the regulated test data in China as an intern to carry out the research work.

[1]Xin Bi, Zhichao Li, Panpan Tong are with the School of Automotive Studies, Tongji University, Shanghai 201804, China (e-mail: bixin@tongji.edu.cn; 2231552@tongji.edu.cn; tongpanpan@tongji.edu.cn).

[2]Yuxuan Xia was with Zenseact, and he is now with the Department of Automation and Perception, Shanghai Jiao Tong University, Shanghai 200240, China. (e-mail:yuxuan.xia@sjtu.edu.cn).

[2]Lijuan Zhang, Yang Chen, Junsheng Fu are with Zenseact, Lindholmspiren 2, Gothenburg 41756, Sweden (e-mail: lijuan.zhang@zenseact.com; yang.chen@zenseact.com; junsheng.fu@zenseact.com).

(a) Image taken from the front-view camera

(b) An illustration of the ego vehicle trajectory

Fig. 1: A challenging scenario in a multilevel road area. In this scenario, the vehicle is driving on the ramp of an elevated road, but the positioning drifts to either the elevated road or the adjacent surface road, making it difficult to achieve accurate map matching.

Existing online map matching methods have inferior performance in complex scenarios, as illustrated in Fig. 1. There are three main challenges in such scenarios: positioning errors, Standard Definition (SD) map inaccuracies and complex road networks. First, vehicle positioning errors can reach tens of meters in urban canyons [2], significantly reducing map matching accuracy. Second, SD map lacks lane-level details and cannot provide high-precision road network geometric data. This leads to the inability to provide the exact boundary geometry of road splits on the map. In addition, the lack of road height information in certain countries makes it not always possible to assist map matching in multilevel road area. Third, incorrect matching is likely to occur at road splits e.g. expressway ramps, where the main road and ramp run adjacent to each other, forming a small included angle. Moreover, solely relying on vehicle positioning and road geometry fails to solve the matching ambiguities regarding whether the vehicle is on elevated roads or underneath them.

In this letter, we present a new online map matching method that can effectively address the above mentioned challenges. Specifically, we leverage visual information including lane marking detections and scenario recognition in the conventional map matching method based on Hidden Markov Model (HMM). The overall framework is illustrated in Fig. 2, and the main contributions include:

- **Online map matching using enriched SD map**: We use an multi-lane tracking method [3] to generate the lane markings, which are then associated with the SD map, forming a lane-level enriched SD map. By leveraging lane marking information from the enriched SD

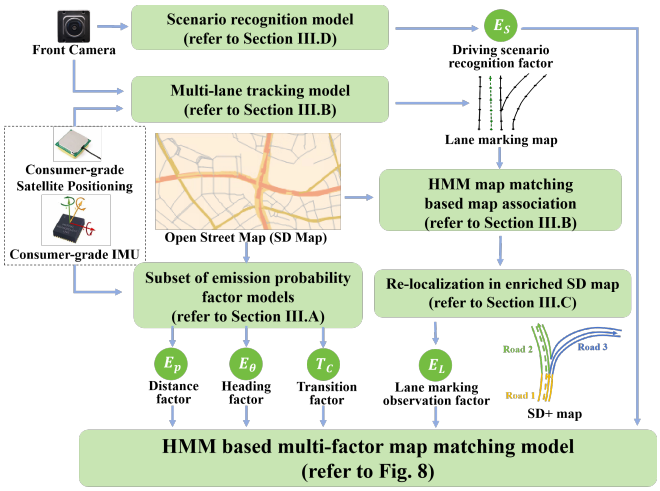

Fig. 2: The overall framework of online map matching in complex road networks using lane markings and scenario recognition.

map as probability factors in the HMM, our proposed method enables re-localization of the vehicle on the map and thereby enhances map matching accuracy at road splits.

- **Integration of driving scenario recognition into HMM**: We incorporate the driving scenario recognition model by OMM-OBDSC [4] into the design of the HMM factors for the online map matching method, enhancing map matching performance in multilevel road areas.
- **Benchmark of online map matching in urban complex road network scenarios**: Extensive tests on the Zenseact Open Dataset [5] and urban roads in Shanghai, China, covering complex road conditions, such as elevated roads, expressway ramps, and ordinary urban roads, show that our proposed method achieves F_1 scores of 98.04% and 94.60% on the Zenseact Open Dataset and test data of multilevel road areas in Shanghai respectively, significantly outperforming benchmark methods.

II. RELATED WORK

Map matching has been an important research area, with some popular solutions proposed in the literature, e.g. the nearest neighbor matching from point to curve [6] and from curve to curve [7], ST-match [8] and the HMM map matching algorithm [9]. The HMM based map matching algorithm has been extensively studied due to its excellent performance. In addition, learning based map matching methods, such as DeepMM [10], L2MM [11], and GraphMM [12] have emerged which model the vehicle trajectories and maps as the inputs of the neural network. However, the mainstream map matching methods solely rely on trajectory information without multi-sensor data integration, resulting in limited performance in complex and dense urban road networks.

In [13], lane-level map matching is performed with the assistance of surrounding lane markings (dashed, solid, etc.) using High Definition (HD) map. But given the limited coverage and high maintenance cost of HD maps, SD maps plays a crucial role for intelligent driving. In [14], SD map and vehicle-mounted perception are used to generate online vectorized HD map representations. In Advanced Driver-Assistance Systems (ADAS), cameras that generate lane markings are being equipped on intelligent vehicles for localization [15]. LaneMatch is proposed in [16] to localize vehicle by matching lane detection outputs with the lane-marking shapes and types extracted offline from satellite images.

In addition to lane markings, road recognition can be also leveraged for map matching. In [17], specific combinations of filters for different operational environments are provided, which can adjust the matching process according to the traffic scenario. In [18], an Elevated Road Network is proposed to address the elevated road recognition problem, which takes speed, satellite SNR and distance to elevated road as input for elevated road recognition. DSCMM [19] and OMM-OBDSC [4] used front-view images for driving scenario recognition to obtain road class probabilities by processing front-view images. In [20] and [21], an Elevation-Aware Unit is proposed to utilize front-view images and IMU data to acquire elevation information for diverse urban roads. While these methods can mitigate errors from elevated roads and ordinary urban roads underneath them, they are less effective for road splits.

This letter presents an online map matching method based on scenario recognition and lane markings, aiming to enhance matching accuracy in complex road networks, especially in multilevel road areas.

III. METHOD

The proposed method extends the traditional HMM based map matching framework. In addition to conventional emission probability estimations, which are typically derived from the distance and included angle between the vehicle trajectory and candidate road segments, our approach leverages front-view camera images to generate lane markings and perform scenario recognition. By incorporating visual context, the method acquires richer semantic information, thereby improving the accuracy of the map matching process.

A. HMM Map Matching Model

1) State Space Model: In the map matching model, the hidden state x_N represents the actual road that the vehicle is on. For example, $x_N = r_i$ indicates that the vehicle is on road r_i at time step N. The perception information, e.g. vehicle positions and front-view images, serve as the observations.

In HMM map matching model, it is assumed that the current state x_N at time step N depends only on the previous state x_{N-1} at time step $N-1$, expressed as

$$P(x_N|x_{N-1}, x_{N-2}, ..., x_0) = P(x_N|x_{N-1}). \quad (1)$$

2) Emission probability factor based on vehicle pose: The main observations at time N are the vehicle position p_N and the vehicle heading angle θ_N, as shown in Fig. 3. Candidate

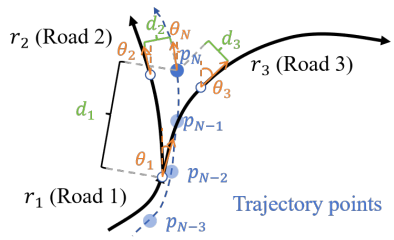

Fig. 3: Schematic diagram of calculating the distance from the vehicle to the road and the road heading angle. In the diagram, p_N represent vehicle positioning points at time N, which form the vehicle trajectory together with p_{N-1}, p_{N-2}, and p_{N-3}. θ_N denotes the vehicle heading angle at time N. Specifically, d_1, d_2, and d_3 are the distances from the vehicle's positioning point p_N to roads r_1, r_2, and r_3, respectively. When a projection point exists on the road, the perpendicular distance is taken; otherwise, the distance to the road endpoint is used. Additionally, θ_1, θ_2, and θ_3 represent the road heading angles at the nearest points from the vehicle to roads r_1, r_2, and r_3, respectively.

roads within a certain area are queried based on the vehicle's current positioning, in the sense that the probability that the vehicle is on a given road decreases as the distance between the vehicle's position and the road increases. We denote the distance between the vehicle position and the i-th candidate road r_i using d_i, which is assumed to be zero-mean Gaussian distributed with standard deviation σ. Then the emission probability factor of distance d_i is given by:

$$p_d(d_i|x_N = r_i) = \mathcal{N}(d_i; 0, \sigma), \tag{2}$$

where $\Delta\theta_i$ is the included angle of vehicle heading θ_N and road heading θ_i ($0° \leq \theta_N, \theta_i \leq 360°$), with

$$\Delta\theta_i = \min\left(|\theta_i - \theta_N|, 360° - |\theta_i - \theta_N|\right), \tag{3}$$

$$p_\theta(\Delta\theta_i|x_N = r_i) \propto \begin{cases} \frac{1+\cos(2\Delta\theta_i)}{2}, & \text{if } \Delta\theta_i < 90°, \\ \varepsilon_1, & \text{otherwise}, \end{cases} \tag{4}$$

where ε_1 is the probability compensation value to deal with potential U-turn and reverse driving behaviors, and in this work it is set to 10^{-4}. It can be seen from Eq. (4) that the probability of the vehicle being on candidate road r_i decreases as $\Delta\theta_i$ increases.

3) Transition Probability Factor Based on Road Connectivity: Roads with connectivity information can be regarded as a directed graph. The transition probability factor depends on the road connectivity, and to compute it we first divide the roads into three categories according to the connection with road r_j: the set R_A consists of the successor roads directly connected to r_j and also r_j itself (i.e., *j=i*), whereas set R_B consists of the roads connected to r_j through other intermediate roads. The transition probability factor from road r_j to road r_i is then given by

$$P_T(x_N = r_i|x_{N-1} = r_j) \propto \begin{cases} 1, & \text{if } r_i \in R_A, \\ e^{-\frac{l_{i,j}}{\gamma}}, & \text{if } r_i \in R_B, \\ \varepsilon_2, & \text{otherwise}, \end{cases} \tag{5}$$

where $l_{i,j}$ is the minimum connected distance between r_i and r_j, γ is the attenuation adjustment factor, and ε_2 is the probability compensation value, which is set to 10^{-4} to deal with potential road transitions that do not conform to traffic regulations.

Fig. 4: An example of the lane markings generated by the multi-lane tracking method. Each red curve represents a tracked lane marking, and the **black dashed curve** represents the vehicle trajectory. The base map for reference is from Google Satellite Map.

4) State Backtracking Using the Viterbi Algorithm: We apply the Viterbi algorithm [22] for online dynamic programming to solve the optimal hidden state sequence of the Hidden Markov Model. Here we use H_N to represent the set of all candidate roads at time N. For each candidate road $r_i \in H_N$ of the state x_N at time N, we use the Viterbi algorithm to calculate the joint probability and find the hidden state sequence with the maximum probability corresponding to each candidate road r_i. The joint probability $P(x_N = r_i, d_i, \Delta\theta_i|x_{N-1})$ of candidate road r_i at time N of the Hidden Markov Model is given by

$$\begin{aligned} &P(x_N = r_i, d_i, \Delta\theta_i|x_{N-1}) \\ &\propto \max_{r_j \in H_{N-1}} \{P(x_{N-1} = r_j, d_j, \Delta\theta_j|x_{N-2}) \\ &\qquad \times P_T(x_N = r_i|x_{N-1} = r_j) \\ &\qquad \times p_d(d_i|x_N = r_i) \times p_\theta(\Delta\theta_i|x_N = r_i)\}. \end{aligned} \tag{6}$$

After computing the unnormlized joint probabilities of $P(x_N = r_i, d_i, \Delta\theta_i|x_{N-1})$ for each $r_i \in H_N$, these values need to be normalized to ensure that the joint probability Eq. (6) is a proper probability function. The optimal matched road r_N^* at time N is given by:

$$r_N^* = \arg\max_{r_i \in H_N} \; P(x_N = r_i, d_i, \Delta\theta_i|x_{N-1}). \tag{7}$$

By backtracking the state of the optimal matched road r_N^* at time N in the Hidden Markov Model, the maximum likelihood state sequence can be obtained, which is the road sequence matched to the vehicle trajectory.

B. The Association of Generated Lane Markings with SD Map

In this work, we adopt the multi-lane tracking method proposed in [3] to generate the lane markings. This method makes use of the lane marking detection points extracted from the camera data to continuously generate and track the lane markings as the vehicle travels. Note that generated lane markings is represented by a set of polylines, where each polyline is compactly parameterized by a sequence of B-spline control points.

An example of the generated lane markings is shown in Fig. 4. With the lane markings in place, the map matching

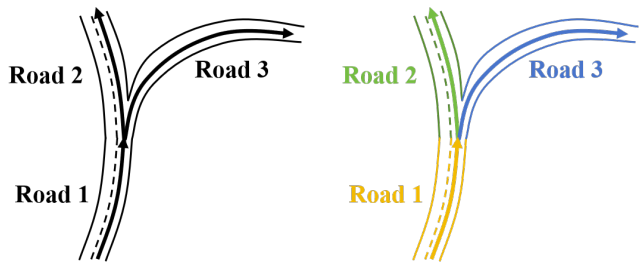

(a) Before association (b) After association

Fig. 5: Schematic diagram of enriched SD map fusion. The **thick polylines**with arrows are the roads of SD map, and the thin solid and dashed polylines represent the solid and dashed lane markings, respectively. In this figure, (a) shows the overlay of lane markings and the SD map in the same coordinate system, and note that there is no correlation between the lane markings and the SD map before performing the association. (b) shows the association result of multiple lane markings with multiple roads. The associated roads and lane markings are marked with the same color In this figure. One road can be associated with multiple lane marking instances, and different parts of one lane marking instance can also be associated with multiple roads with different probabilities.

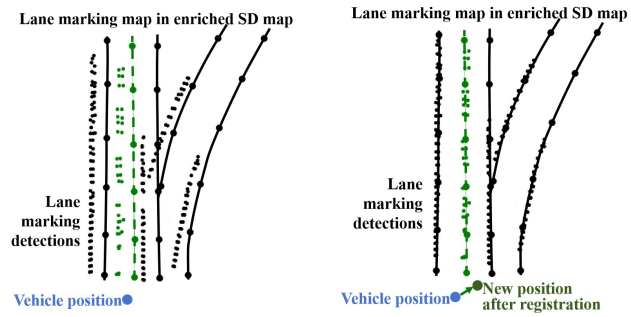

(a) Before registration (b) After registration

Fig. 6: The process of lane marking ICP registration. The points in this figure are from the lane marking detection extracted from the front-view camera, and the polylines are from the enriched SD map. The green parts represent the dashed lanes, and the **black parts** represent the solid lanes. In this figure, (a) shows the lane marking detection point cloud and the lane markings from enriched SD map before registration. (b) shows the lane marking detection point cloud and the lane markings from enriched SD map after registration. It can be seen that after performing ICP registration, the vehicle can re-localize itself in enriched SD map.

model described in Section III.A can be used to associate the tracked lane markings with the roads in the map.

Denote the set of tracked lane markings as $L = \{l_j | j = 1, 2, ..., m\}$, where m represent the total number of lane markings. The lane markings in the form of B-splines output by the multi-lane tracking method can be sampled to obtain discrete directed coordinate point sequences. Assume that each lane marking contains n sampling points, denoted as $l_j = \{l_{j,1}, l_{j,2}, ..., l_{j,n}\}$. Bring the coordinates $l_{j,k}$ and the heading angle $\theta_{j,k}$ of the sampled lane marking points into the model in Section III.A. The key is to adjust the value of the parameter σ to fit the perpendicular distance distribution of the vehicle from the lane markings. We represent the association and subordination between $l_{j,k}$, l_j and r_i in the SD map in a simplified manner using a mapping function $\mathcal{M}_1(l_{j,k}) = r_i$ and $\mathcal{M}_2(l_j) = r_i$ respectively. Then based on the map matching algorithm, $P_m(\mathcal{M}_1(l_{j,k}) = r_i)$, the probability of each tracked lane marking sampling point $l_{j,k}$ being matched to each candidate road r_i can be calculated. In addition, by tracing back from the optimal matching sequence, the probability of each sampled point of the lane markings being matched to other roads can be obtained. The maximum value of these probabilities of being matched to each candidate road as the association probability between l_j and r_i can be obtained as

$$P(\mathcal{M}_2(l_j) = r_i) = \max_{k=1,2,...,n} P(\mathcal{M}_1(l_{j,k}) = r_i). \quad (8)$$

An example of the association between the lanes and the roads is shown in Fig. 5. Through associating the lane markings with the roads, a lane-level enriched SD map is formed, and therefore the online map matching of the vehicle passing through the mapped area can be assisted by better map information.

C. Emission Probability Factor of Lane Marking Detection

Since there are positioning biases in each vehicle travel, in order to judge the current lane where the vehicle is located and obtain the information of the surrounding lane markings, we adopt the Iterative Closest Point (ICP) algorithm [23] to locate the vehicle in the lane-level enriched SD map. The registration loss L_r between the vehicle lane marking detection point and the points in the enriched SD map during the nearest neighbor point query is given by

$$L_r(p_v, p_m) = \sqrt{(x_v - x_m)^2 + (y_v - y_m)^2 + L_{type}^2}, \quad (9)$$

$$L_{type} = \begin{cases} 0, & \text{if } t_v = t_m, \\ f_{type}, & \text{if } t_v \neq t_m, \end{cases} \quad (10)$$

where t_v and t_m are, respectively, the lane marking type of the vehicle lane marking detection point and the lane marking type of the down-sampled point in the enriched SD map; L_{type} is the registration loss of the lane marking type, and $L_{type} = f_{type}$ if $t_v \neq t_m$. A larger value of f_{type} indicates a greater confidence in the classification accuracy of the lane marking detection algorithm. A comparison of vehicle position before and after registration is shown in Fig. 6.

After the lane markings were associated with the SD map in Section III.B, an enriched SD map was formed. By using the positions and included angles of all the lane markings L_N near the position of the vehicle at time N, the projection points of the vehicle position onto the adjacent lane markings are calculated, and the distance $d_{lane,j}$ between the vehicle and the lane markings as well as the heading included angle $\Delta\theta_j = |\theta_{lane,j} - \theta_N|$ are obtained. Then, combined with the association probability between the lane markings and the roads, the lane marking detection probability factor of the vehicle for each candidate road can be calculated as

$$\begin{aligned} P_L(x_N = r_i | L_N) \propto \sum_{l_j \in L_N} P_m(\mathcal{M}_2(l_j) = r_i)) \\ \times \mathcal{N}(d_i; 0, \sigma) \times p_\theta(\Delta\theta_j | x_N = r_i). \end{aligned} \quad (11)$$

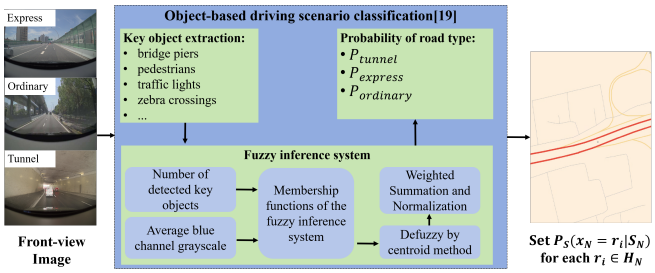

Fig. 7: The process of deriving driving scenario recognition probability factors from the front-view image. The driving scenario recognition model from OMM-OBDSC [4] is used to process the front-view image to obtain the probabilities of the vehicle being on the different roads. The method first uses YOLO object detector [25], which has been trained to detect the typical objects of different road types, including bridge piers, pedestrians, traffic lights, zebra crossings, non-motor vehicles, etc. Next, the average grayscale value of the blue channel of the image is calculated as an input of the fussy inference system. In the end, the emission probability factors of driving scenario recognition are generated for each candidate road.

D. Emission Probability Factor of Driving Scenario Recognition

In the complex urban road network, different types of roads are closely adjacent in the three-dimensional space. This makes it difficult for the vehicle to effectively distinguish the actual matched road. To address this problem, we make use of driving scenario recognition in the calculation of the emission probability factor. In this work, we use the driving scenario recognition model from OMM-OBDSC [4] to process the images from the front-view camera. And by doing so we can obtain the probabilities that the scenario belong to ordinary urban roads, expressways, and tunnels, denoted using $P_{ordinary}$, $P_{express}$, P_{tunnel}, respectively as shown in Fig. 7. We refer the readers to [24] for more details of the driving scenario recognition module. Then, the output of the above OBDSC model is added as a probability factor to the Hidden Markov Model, which is given by

$$P_S(x_N = r_i|S_N) = \begin{cases} P_{ordinary}, & \text{if } r_i \in R_N, \\ P_{express}, & \text{if } r_i \in R_E, \\ P_{tunnel}, & \text{if } r_i \in R_T, \end{cases} \tag{12}$$

where S_N is the overall scenario information captured from the front-view image, R_N is the set consisting of ordinary urban roads in the map, R_E is the set consisting of elevated road or expressways in the map, and R_T is the set consisting of tunnel roads.

E. Improved Hidden Markov Model Probability Factor Graph

After the incorporation of enriched SD map and driving scenario recognition, the complete Hidden Markov Model with multiple probability factors is shown in Fig. 8. The joint probability of the state x_N at time N of the Hidden

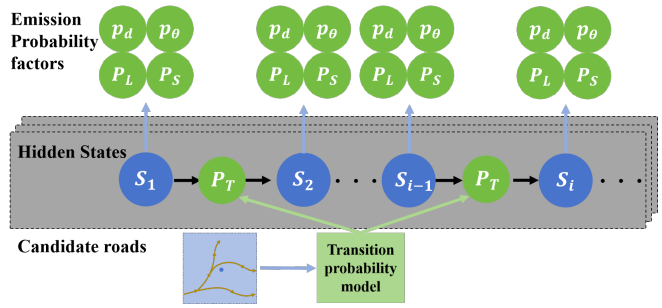

Fig. 8: HMM with multiple probability factors.

Fig. 9: An overview of the driving scenarios for testing the map matching algorithm.

Markov Model can be finally expressed as

$$\begin{aligned} &P(x_N = r_i, d_i, \Delta\theta_i|x_{N-1}) \\ &\propto \max_{r_j \in H_{N-1}} \{P(x_{N-1} = r_j, d_j, \Delta\theta_j|x_{N-2}) \\ &\qquad \times P_T(x_N = r_i|x_{N-1} = r_j) \\ &\qquad \times p_d(d_i|x_N = r_i) \times p_\theta(\Delta\theta_i|x_N = r_i) \\ &\qquad \times P_L(x_N = r_i|L_N) \times P_S(x_N = r_i|S_N)\}. \end{aligned} \tag{13}$$

Then the Viterbi algorithm mentioned in Section III.A can be used to find the maximum likelihood state sequence, which are the matched roads corresponding to the vehicle trajectory.

IV. EXPERIMENTS

The SD map used in this work is OpenStreetMap (OSM) [27]. Subsequent tests are carried out on Drives of Zenseact Open Dataset [5] and road tests covering 102.6 kilometers in Shanghai, China. The test scenarios cover various types of roads ranging from expressways to rural roads. Examples of these scenarios are shown in Fig. 9.

A. Map Matching Evaluation Metrics

In this work we use *MatchRate*, *Precision*, *Recall* and F_1 score for performance evaluation.

The *MatchRate* is defined as the proportion of correctly matched trajectory points $N_{correct}$ among all trajectory points N_{all}:

$$MatchRate = \frac{N_{correct}}{N_{all}}, \tag{14}$$

We let *TP* be the true positives, *FP* be the false positives, *FN* be the false negatives. Then the *Precision* is the fraction of relevant instances among the retrieved instances, expressed as $Precision = \frac{TP}{TP+FP}$. The *Recall* is the fraction of relevant instances that have been retrieved over the total amount of relevant instances, expressed as $Recall =$

TABLE I
RESULTS ON DRIVES OF ZENSEACT OPEN DATASET [5]

Method	Positioning inputs [5]	*MatchRate* (%)	↑	*Precision* (%)	↑	*Recall* (%)	↑	F_1 score (%)	↑
Nearest neighbor [6]	GNSS	91.43		89.06		89.43		89.25	
Nearest neighbor [6]	GNSS+IMU	92.48		90.10		90.51		90.30	
Nearest neighbor [6]	OxTS RT3000	95.10		93.49		94.10		93.80	
Online HMM [9]	GNSS	96.51		95.30		95.41		93.73	
AMM [26]	GNSS	94.39		93.88		94.07		93.97	
Online HMM + OBDSC [4]	GNSS	96.97		96.08		96.18		96.13	
Proposed method	GNSS	98.26		97.83		97.92		97.87	
Proposed method	GNSS+IMU	**98.35**		**98.00**		**98.08**		**98.04**	

↑ The upper arrow denotes that better performance is registered with higher value.

TABLE II
RESULTS ON TEST DATA OF MULTILEVEL ROAD AREAS IN SHANGHAI

Method	Positioning inputs [5]	*MatchRate* (%)	↑	*Precision* (%)	↑	*Recall* (%)	↑	F_1 score (%)	↑
Nearest neighbor [6]	GNSS	64.53		43.10		43.81		43.45	
Nearest neighbor [6]	GNSS+IMU	65.14		44.65		45.68		45.16	
Nearest neighbor [6]	OxTS RT3000	78.09		65.05		65.46		65.25	
Online HMM [9]	GNSS	74.56		62.90		63.78		63.33	
AMM [26]	GNSS	67.47		66.84		66.89		66.87	
Online HMM + OBDSC [4]	GNSS	89.63		88.23		89.27		88.75	
Proposed method	GNSS	91.60		93.85		94.57		94.21	
Proposed method	GNSS+IMU	**92.95**		**93.99**		**95.21**		**94.60**	

$\frac{TP}{TP+FN}$. In the context of map matching, the *Precision* and *Recall* can be, respectively, defined as

$$Precision = \frac{L_{correct}}{L_{mm}}. \tag{15}$$

$$Recall = \frac{L_{correct}}{L_{gt}}. \tag{16}$$

where L_{gt} is the length of the ground truth trajectory, L_{mm} is the length of the map matching trajectory, and $L_{correct}$ is the length of the correct overlapping road segments between the map matching trajectory and ground truth trajectory.

The F_1 score is defined using *Precision* and *Recall* as

$$F_1 = \frac{2 \times Precision \times Recall}{Precision + Recall}. \tag{17}$$

B. Test on Drives of Zenseact Open Dataset

In order to evaluate the effectiveness of the proposed method in the online navigation and positioning function, we conducted tests on Drives of Zenseact Open Dataset, which covers various road types in Sweden and France.

The comparison of results between our proposed method and other methods is shown in Table I. First we apply nearest neighbor matching (point-to-curve [6]) using three different positioning inputs: standalone GNSS, fused GNSS/IMU, and the high-precision OxTS RT3000 (refer to [5] for device specifications). All positioning data were down-sampled to 1 FPS to ensure consistency with GNSS sampling rates. When used as inputs for map matching, the F_1 score improved by 1.05% and 4.55%, respectively. However, these improvements remain insufficient to reach the performance level of mainstream map matching algorithms. This suggests that enhancing positioning accuracy alone is inadequate to fully address the challenges of map matching. Consequently, for a more comprehensive comparison, we evaluate our proposed method against four other benchmark methods. According to the experimental results, our proposed method achieved an average *MatchRate*, *Precision*, *Recall*, F_1 score of 98.35%, 98.00%, 98.08% and 98.04%, respectively. All evaluation metrics are superior to those of the comparative methods.

Fig. 10: The test trajectories are shown on the SD map (OpenStreetMap[27]) within the multilevel road areas in Shanghai. The blue polylines represent the trajectories.

In order to further test the performance of our proposed method in more complex road networks, we have conducted experiment on test data of multilevel road areas in Shanghai.

C. Test on Multilevel Road Areas in Shanghai

We conducted the data collection experiment using a vehicle with the same sensor configuration as that of the

TABLE III
ABLATION EXPERIMENTS ON BOTH DATASETS

Dataset	Model	*MatchRate* (%) ↑	*Precision* (%) ↑	*Recall* (%) ↑	F_1 score (%) ↑
Zenseact Open Dataset [5] (Drives)	P_L and P_S ablated (Baseline)	97.58	96.72	96.83	96.77
	$+P_S$ [1]	97.95 (+0.37)	97.28 (+0.56)	97.38 (+0.55)	97.33 (+0.56)
	$+P_L$ [2]	98.16 (+0.58)	97.69 (+0.97)	97.79 (+0.96)	97.74 (+0.97)
	$+P_S + P_L$(Proposed method)	**98.26 (+0.68)**	**97.83 (+1.11)**	**97.92 (+1.09)**	**97.87 (+1.10)**
Test data of multilevel road areas in Shanghai	P_L and P_S ablated (Baseline)	75.41	65.89	66.75	66.32
	$+P_S$	90.38 (+14.97)	92.31 (+26.42)	93.18 (+26.43)	92.74 (+26.42)
	$+P_L$	82.95 (+7.54)	78.87 (+12.98)	79.58 (+12.83)	79.22 (+12.90)
	$+P_S + P_L$(Proposed method)	**91.60 (+16.19)**	**93.85 (+27.96)**	**94.57 (+27.82)**	**94.21 (+27.89)**

[1] Emission probability factor of driving scenario recognition
[2] Emission probability factor of lane marking detection

Zenseact Open Dataset [5]. The trajectory in China covers the multilevel road areas in Shanghai, which includes different road types such as road splits in expressway, the elevated roads and ordinary urban roads underneath them, and tunnels. The trajectory of the tested scenario is shown in Fig. 10. Further verification has been carried out on the driving data totaling 8680 seconds in duration and covering an accumulated distance of 102.6 kilometers. This is used to verify the effectiveness of the method proposed in this letter for matching in complex urban road areas. The test results are shown in Table II. The online map matching task in Shanghai is more challenging due to the city's complex, dense, and multi-level road network, compared to the driving data from the Zenseact Open Dataset, which was captured in Europe.

Since the elevated roads and ordinary urban roads underneath them are parallel and adjacent in Shanghai multilevel road area, the vehicles can easily fail to distinguish whether they have entered or left the elevated road through the ramp. Therefore, the emission probability factor of driving scenario recognition P_S and the emission probability factor of lane marking detection P_L play a very significant role in the map matching algorithm. Notably, they can prevent the vehicle from being wrongly matched to the surface road while driving on the elevated road, or vice versa. The experiments show that our proposed method outperforms the benchmarking methods by a large margin on test data of multilevel road areas in Shanghai.

D. Ablation study

To more precisely assess the contributions of each module to the evaluation metrics, we carried out ablation experiments relying solely on GNSS to ensure a fair comparison. The outcomes of these experiments are presented in Table III.

An examination of the ablation experiment results in Table III reveals that both the emission probability factor of driving scenario recognition, denoted as P_S, and the emission probability factor of lane marking detection, denoted as P_L, have a positive impact on the matching evaluation metrics. In the driving scenarios of the Zenseact Open Dataset, P_L plays a more significant role. Incorporating P_L can effectively enhance the evaluation metrics, particularly when the vehicle is required to differentiate the correct road at road junctions.

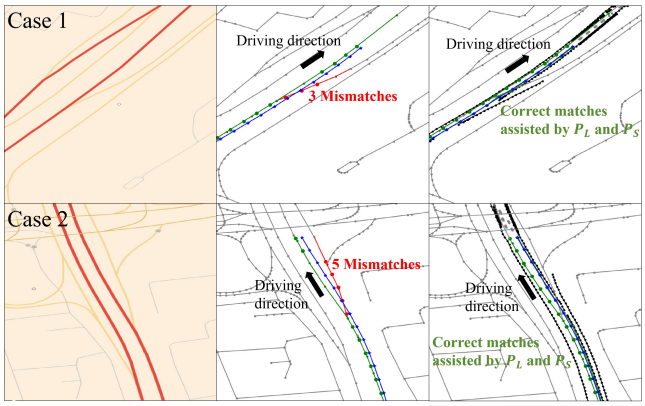

(a) SD Map colored by different road class (b) Baseline in Table III (c) Proposed method

Fig. 11: Improvements of online map matching in the case of road splits. Our proposed method enables vehicles to be localized on the correct roads with the aid of enriched SD map, so that addresses the issue of incorrect map matching due to trajectory deviations. In (a), the SD map utilized by the map matching algorithm is visualized. In (b), the matching errors that occurred after ablating P_S and P_L are illustrated. The solid gray curve represents the roads in the SD map. The solid blue polyline depict the vehicle's trajectory, while the blue stars indicate discrete trajectory points. The solid green polylines denote the correctly matched roads, and the green circles represent correct road projection points. Conversely, the solid red polylines illustrate the incorrectly matched roads, along with the red circles indicating incorrect road projection points. In (c), the accurate matching results generated by our proposed method are shown. The enriched SD map is shown, and both P_S and P_L are employed in the map matching process. The **solid black polylines** correspond to solid lane markings, while the gray dashed polylines represent dashed lane markings.

In the tests conducted in the multilevel road areas of Shanghai, the emission probability factor of driving scenario recognition, P_S, plays a more prominent role. When both of these factors are removed from the method, the *MatchRate* drops to 75.41%, and the F_1 score drops to 66.32%. When only P_S is introduced, the F_1 score experiences a 26.42% increase, reaching 92.74%. Conversely, when only P_L is added, and the F_1 score rises to 79.22%. However, both of these values are lower than the F_1 score of 94.21% achieved by the proposed method before ablation.

Fig. 11 and Fig. 12 shows the improvements of our proposed method in several scenarios. This comparison un-

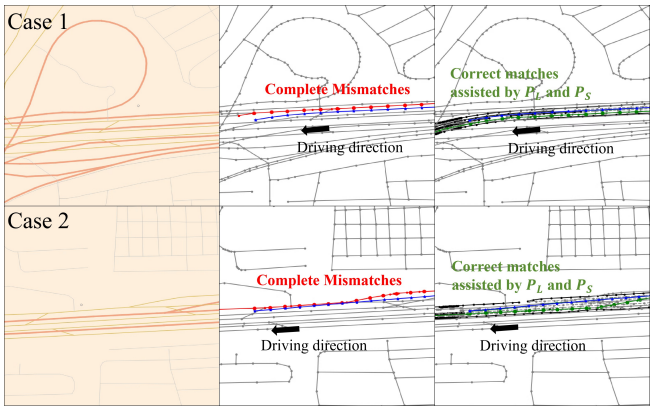

(a) SD Map colored by different road class (b) Baseline in Table III (c) Proposed method

Fig. 12: Improvements of online map matching in the case of multilevel road areas. Our proposed method effectively enables vehicles to be localized on the correct elevated roads with the aid of driving scenario recognition.

derscores the significance of the emission probability factor of driving scenario recognition P_S and the emission probability factor of lane marking detection P_L in distinguishing between elevated roads and ordinary urban roads, as well as in differentiating the split roads of expressways.

V. CONCLUSIONS

In this work, we propose a HMM-based multi-factor online map matching method that integrates lane markings to form the enriched SD map and driving scenario recognition using on-board camera input. By incorporating visual context, the method enhances semantic understanding of the driving environment, leading to improved accuracy in online map matching. Extensive evaluations on the Zenseact Open Dataset and in complex road networks in Shanghai demonstrate that our approach outperforms existing methods, particularly in challenging scenarios such as road splits and multilevel road areas.

ACKNOWLEDGEMENT

The authors from Tongji University were funded in part by the National Key R&D Program of China under Grant 2022YFE0117100. This work was completed through the collaboration between Tongji University and Zenseact. The cooperation brought together complementary expertise and resources, facilitating the smooth progress of our research. We are deeply indebted to both institutions for their contributions to this work.

REFERENCES

[1] L. Mendiboure, M. L. Benzagouta, D. Gruyer, *et al.*, "Operational design domain for automated driving systems: Taxonomy definition and application," in *2023 IEEE Intelligent Vehicles Symposium (IV)*, 2023, pp. 1–6.

[2] D. Weng, M. Cai, W. Chen, *et al.*, "Gnss fault detection and exclusion (fde) under sidewalk constraints for pedestrian localization in urban canyons," *IEEE Transactions on Intelligent Transportation Systems*, vol. 25, no. 9, pp. 11 168–11 179, 2024.

[3] Y. Xia, E. Stenborg, J. Fu, *et al.*, "Bayesian simultaneous localization and multi-lane tracking using onboard sensors and a sd map," *2024 27th International Conference on Information Fusion (FUSION)*, pp. 1–8, 2024.

[4] H. Wu, S. Huang, C. Fu, *et al.*, "Online map-matching assisted by object-based classification of driving scenario," *International Journal of Geographical Information Science*, vol. 37, no. 8, pp. 1872–1907, 2023.

[5] M. Alibeigi, W. Ljungbergh, A. Tonderski, *et al.*, "Zenseact open dataset: A large-scale and diverse multimodal dataset for autonomous driving," in *2023 IEEE/CVF International Conference on Computer Vision (ICCV)*, 2023, pp. 20 121–20 131.

[6] C. E. White, D. Bernstein, and A. L. Kornhauser, "Some map matching algorithms for personal navigation assistants," *Transportation Research Part C: Emerging Technologies*, vol. 8, no. 1, pp. 91–108, 2000.

[7] K. P. Sharma, R. C. Pooniaa, and S. Sunda, "Map matching algorithm: Curve simplification for frechet distance computing and precise navigation on road network using rtklib," *Cluster Computing-The Journal of Networks, Software Tools and Applications*, vol. 22, no. 6, pp. 13 351–13 359, Nov. 2019.

[8] Y. Lou, C. Zhang, Y. Zheng, *et al.*, "Map-matching for low-sampling-rate gps trajectories," in *Proceedings of the 17th ACM SIGSPATIAL International Conference on Advances in Geographic Information Systems*, Seattle, Washington: Association for Computing Machinery, 2009, pp. 352–361.

[9] P. Newson and J. Krumm, "Hidden markov map matching through noise and sparseness," in *Proceedings of the 17th ACM SIGSPATIAL International Conference on Advances in Geographic Information Systems*, Seattle, Washington: Association for Computing Machinery, 2009, pp. 336–343.

[10] J. Feng, Y. Li, K. Zhao, *et al.*, "Deepmm: Deep learning based map matching with data augmentation," *IEEE Transactions on Mobile Computing*, vol. 21, no. 7, pp. 2372–2384, 2022.

[11] L. Jiang, C. Chen, and C. Chen, "L2mm: Learning to map matching with deep models for low-quality gps trajectory data," *ACM Transactions on Knowledge Discovery from Data*, vol. 17, pp. 1–25, 2022.

[12] Y. Liu, Q. Ge, W. Luo, *et al.*, "Graphmm: Graph-based vehicular map matching by leveraging trajectory and road correlations," *IEEE Transactions on Knowledge and Data Engineering*, vol. 36, no. 1, pp. 184–198, 2024.

[13] A. Hansson, E. Korsberg, R. Maghsood, *et al.*, "Lane-level map matching based on hmm," *IEEE Transactions on Intelligent Vehicles*, vol. 6, no. 3, pp. 430–439, 2021.

[14] H. Zhang, D. Paz, Y. Guo, *et al.*, "Enhancing online road network perception and reasoning with standard definition maps," in *IROS*, 2024, pp. 1086–1093.

[15] A. Welte, P. Xu, P. Bonnifait, *et al.*, "Improved data association using buffered pose adjustment for map-aided localization," *IEEE Robotics and Automation Letters*, vol. 5, no. 4, pp. 6334–6341, 2020.

[16] M. He and R. R. Rajkumar, "Lanematch: A practical real-time localization method via lane-matching," *IEEE Robotics and Automation Letters*, vol. 7, no. 2, pp. 4408–4415, 2022.

[17] X. Kong and J. Yang, "A scenario-based map-matching algorithm for complex urban road network," *Journal of Intelligent Transportation Systems*, vol. 23, no. 6, pp. 617–631, 2019.

[18] X. Zhang, H. Xu, J. Yang, *et al.*, "Elevated road network: A metric learning method for recognizing whether a vehicle is on an elevated road," in *Proceedings of the 29th ACM International Conference on Information & Knowledge Management*, Virtual Event, Ireland: Association for Computing Machinery, 2020, pp. 2925–2932.

[19] C. Fu, S. Huang, Y. Tang, *et al.*, "A real-time map matching method for road network using driving scenario classification," *Acta geodaetica et Cartographica Sinica*, vol. 050, no. 011, pp. 1617–1627, 2021.

[20] J. Tang, S. Zheng, B. Yu, *et al.*, "Haum3: A height aware urban map matching mechanism," in *Mobile and Ubiquitous Systems: Comput-*

ing, Networking and Services, Cham: Springer Nature Switzerland, 2024, pp. 505–525.

[21] J. Tang, S. Zheng, B. Yu, *et al.*, "Elevation-aware map matching model leveraging transfer learning in sparse data conditions," *IEEE Transactions on Intelligent Transportation Systems*, vol. 26, no. 3, pp. 3724–3737, 2025.

[22] G. Forney, "The viterbi algorithm," *Proceedings of the IEEE*, vol. 61, no. 3, pp. 268–278, 1973.

[23] P. Besl and N. D. McKay, "A method for registration of 3-d shapes," *IEEE Transactions on Pattern Analysis and Machine Intelligence*, vol. 14, no. 2, pp. 239–256, 1992.

[24] M. N. Sharath, N. R. Velaga, and M. A. Quddus, "A dynamic two-dimensional (d2d) weight-based map-matching algorithm," *Transportation Research Part C: Emerging Technologies*, vol. 98, no. JAN. Pp. 409–432, 2019.

[25] J. Redmon, S. Divvala, R. Girshick, *et al.*, "You only look once: Unified, real-time object detection," in *2016 IEEE Conference on Computer Vision and Pattern Recognition (CVPR)*, 2016, pp. 779–788.

[26] H. Hu, S. Qian, J. Ouyang, *et al.*, "Amm: An adaptive online map matching algorithm," *IEEE Transactions on Intelligent Transportation Systems*, vol. 24, no. 5, pp. 5039–5051, 2023.

[27] M. Haklay and P. Weber, "Openstreetmap: User-generated street maps," *IEEE Pervasive Computing*, vol. 7, no. 4, pp. 12–18, 2008.